

## Research Article

# Influence of Circumferential Placement Position of Guide Vanes on Performance and Dynamic Characteristics of Nuclear Reactor Coolant Pump

Xiaorui Cheng <sup>1,2</sup>, Boru Lv,<sup>1</sup> Chenying Ji,<sup>3</sup> Ningning Jia,<sup>1</sup> and Dorah N<sup>1</sup>

<sup>1</sup>College of Energy and Power Engineering, Lanzhou University of Technology, Lanzhou 730050, China

<sup>2</sup>Key Laboratory of Fluid Machinery and Systems of Gansu Province, Lanzhou 730050, China

<sup>3</sup>Gongzui Hydropower Plant, Guo Dian Dadu River Hydropower Development Co, Leshan 614900, China

Correspondence should be addressed to Xiaorui Cheng; [cxr168861@sina.com](mailto:cxr168861@sina.com)

Received 10 June 2019; Accepted 3 October 2019; Published 29 February 2020

Academic Editor: Jefferson L. M. A. Gomes

Copyright © 2020 Xiaorui Cheng et al. This is an open access article distributed under the Creative Commons Attribution License, which permits unrestricted use, distribution, and reproduction in any medium, provided the original work is properly cited.

In order to study the influence of the circumferential placement position of the guide vane on the flow field and stress-strain of a nuclear reactor coolant pump, the CAP1400 nuclear reactor coolant pump is taken as the research object. Based on numerical calculation and test results, the influence of circumferential placement position of the guide vane on the performance of the nuclear reactor coolant pump and stress-strain of guide vanes are analyzed by the unidirectional fluid-solid coupling method. The results show that the physical model and calculation method used in the study can accurately reflect the influence of the circumferential placement position of the guide vane on the nuclear reactor coolant pump. In the design condition, guide vane position has a great influence on the nuclear reactor coolant pump efficiency value, suction surface of the guide vane blade, and the maximum equivalent stress on the hub. However, it has a weak effect on the head value, pressure surface of the guide vane blade, and the maximum equivalent stress on the shroud. When the center line of the outlet diffuser channel of the case is located at the center of the outlet of flow channel of the guide vane, it is an optimal guide vane circumferential placement position, which can reduce the hydraulic loss of half of the case. Finally, it is found that the high stress concentration area is at the intersection of the exit edge of the vane blade and the front and rear cover, and the exit edge of the guide vane blade and its intersection with the front cover are areas where the strength damage is most likely to occur. This study provides a reference for nuclear reactor coolant pump installation, shock absorption design, and structural optimization.

## 1. Introduction

The impeller, guide vane, and volute are the key overcurrent components of the nuclear reactor coolant pump. The guide vanes, located behind the impeller and in front of the volute, play an important role in the pump. Their function is to convert the velocity energy of the impeller outlet fluid into pressure energy, eliminate its rotational component, and evenly introduce the fluid into the volute. Therefore, the guide vane has a pivotal status in improving the hydraulic performance of the nuclear reactor coolant pump and reducing the hydraulic loss in the pump. The impeller is a rotating component, and the guide vane and the volute are

stationary components, and the rotor-stator interaction between impeller and guide vane and the relative position of the guide vane and center of the annular case outlet diffuser channel will all affect the comprehensive performance of the nuclear reactor coolant pump. Scholars have done a lot of research on the relevant content of the circumferential arrangement of the guide vanes. For example, Deng Jia et al. [1], taking a single-stage centrifugal pump with low specific speed as the object, researched the effect of different timing positions of the front vane relative to the radial vane on the performance of the pump, and the results showed that the time sequence position has an effect on the vibration characteristics and comprehensive characteristics of

centrifugal pumps. Lu Jinling et al. [2], taking the centrifugal pump with inducer as the object, studied the influence of the clocking position of the inducer relative to the impeller on the hydraulic performance of the pump, and the results showed that the cavitation performance of the centrifugal pump is related to the clocking position. Zhao Ben et al. [3], taking a combined compressor as the object, studied the correlation among the stator blade wake, the interference frequency, and the clocking position of the rotor blade. Cheng Xiaorui et al. [4, 5], taking a nuclear reactor coolant pump as the object, studied the influence of the circumferential position of the guide vane on its pressure fluctuation and the radial force of the impeller. Liu and Xu [6] focused on the high-speed centrifugal compressor and analyzed the corresponding relationship between the internal flow field in the compressor stage and the different starting positions of the splitter blades. Scholars have also carried out a series of studies on the influence of structural parameters of the nuclear reactor coolant pump or mixed-flow pump on its internal flow characteristics. For example, Posa et al. [7] calculated the unsteady flow field in the mixed-flow pump. It was pointed out that the vortex originated from the back of the impeller blade. Yuan et al. [8] studied the influence of different pressure water chamber widths of a nuclear reactor coolant pump on its performance. Jin et al. [9] studied the influence of different blade wrap angles and relative positions of the outlet edge of a guide vane on the hydraulic performance of a nuclear reactor cooling pump. Poullikkas [10] studied the internal flow law of nuclear reactor coolant pumps under two-phase flow.

However, there are a few research studies on the influence of guide vane circumferential position on the hydraulic performance and dynamic characteristics of nuclear reactor coolant pumps. This paper uses the self-developed nuclear reactor coolant pump model as the object and adopts the unidirectional fluid-solid coupling method; based on numerical simulation and test, the influence of guide vane circumferential position on its performance and dynamic characteristics is analyzed.

## 2. Numerical Model and Scheme Design

**2.1. Numerical Model.** In this study, the CAP1400 nuclear reactor coolant pump is taken as the research object. In view of the complex structure and large size of the prototype nuclear reactor coolant pump, if the prototype pump is used for numerical analysis, it will inevitably lead to higher cost of numerical calculation and longer cycle. Therefore, according to the similarity theory, the prototype pump parameters are converted into model pump parameters for numerical analysis and test verification. Considering the distortion rate of hydraulic performance from the prototype pump to the model pump and the numerical cost of the model pump, the scaling ratio  $\psi = 0.4$  [11] is adopted. The structure of the prototype pump is shown in Figure 1(a). According to the similarity theory, the design parameters of the model pump are given in Table 1. The impeller material is duplex stainless steel 2507, with a density of  $\rho = 8\,030\text{ kg/m}^3$ , elastic modulus of  $E = 2.00e + 11\text{ Pa}$ , and Poisson's ratio  $\gamma = 0.3$ ;

pump shaft material 45Cr, with a density of  $\rho = 7\,820\text{ kg/m}^3$ , elastic modulus of  $E = 2.09e + 11\text{ Pa}$ , and Poisson's ratio  $\gamma = 0.269$  [12].

The model is built on the premise that the flow passage components of the nuclear reactor coolant pump are unchanged, and different schemes are established by changing the circumferential placement position of the guide vanes. Because the number of guide vanes in the nuclear reactor coolant pump model is 18, the thickness of guide vane blade makes the circumferential angle between two adjacent guide vane blades about  $18^\circ$ . Therefore, this paper designs seven guide vane layout schemes on the scale of  $3^\circ$ . Figure 1(b) is a schematic diagram of the meridian plane of the model pump, in which A-A' is the center section of the guide vane outlet. Figure 1(c) is a schematic diagram of the circumferential placement position of guide vanes on the A-A' section. In Figure 1(c), the straight line  $ob$  is the line passing through the origin  $o$  and  $b'$  points ( $b'$  points are the intersection points of the pressure surface of guide vane blade 1 and the hub). The circumferential angle of the guide vane is defined as the included angle between the straight line  $ob$  and the  $y$  axis, and the initial position is defined when  $\alpha = 0^\circ$ . The guide vanes are rotated counterclockwise from the initial position. Seven kinds of guide vane circumferential position layout schemes,  $\alpha = 0^\circ, 3^\circ, 6^\circ, 9^\circ, 12^\circ, 15^\circ$ , and  $18^\circ$ , are corresponded, respectively. The validity of the two schemes of  $\alpha = 0^\circ$  and  $6^\circ$  is verified by testing.

**2.2. Grid Generation.** The fluid domain of the nuclear reactor coolant pump consists of an inlet section, impeller, clearance between stator and rotor, guide vane, volute, and outlet section. In order to ensure the accuracy of numerical results, the inlet and outlet pipelines of model pumps are extended appropriately. A structured hexahedral mesh is used to divide the whole fluid domain. The boundary layer mesh is added to all the boundary layers, and the mesh quality is improved by using reconfigurable grid. The mesh generation of the main components of the fluid domain is shown in Figures 2(a)–2(d). Considering that the grid density has a great influence on the numerical results, different grid numbers are selected to verify the grid independence of the fluid domain of the model pump at  $\alpha = 0^\circ$ . The results are shown in Figure 2(e). As can be seen from Figure 2(e), when the number of fluid domain grids is more than 7.21 million, the mesh density is further increased and the head and efficiency values of the model pump are changed within 1%. Considering the need of this study and the calculation workload, a total of 7.21 million grid models are finally selected.

**2.3. Numerical Calculation Method.** The fluid domain calculation uses ANSYS FLUENT to complete the iterative solution of steady value. The governing equation adopts the incompressible Reynolds time-averaged N-S equation, and the discrete of the diffusion term adopts the second-order center difference scheme. Considering the convergence performance of the data, the other terms are all first-order upwind scheme [13]. Because of the existence of rotational

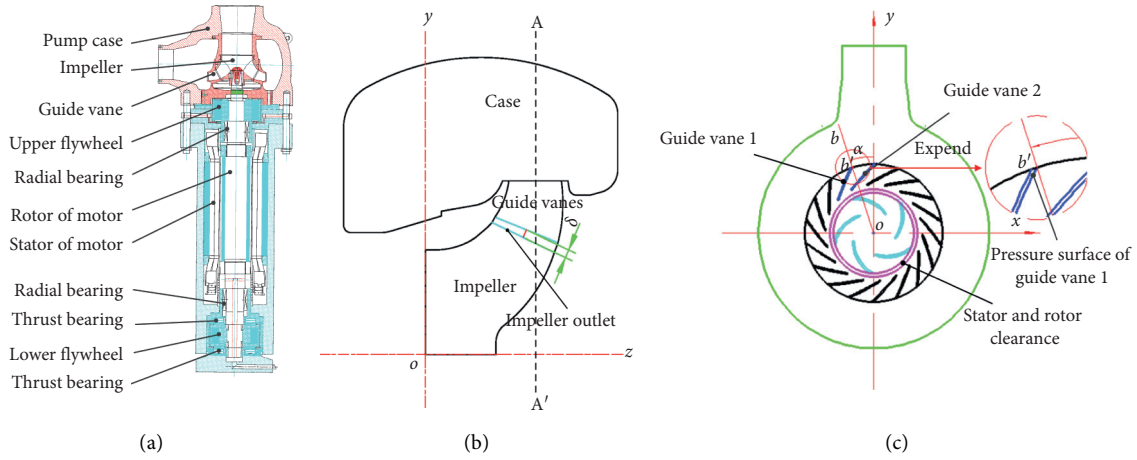


FIGURE 1: Schematic diagram of calculation scheme. (a) structural sketch of the prototype pump. (b) A-A' section position diagram, (c) circumferential placement position.

TABLE 1: Main performance parameters of the model pump.

Parameters	Numerical value
Design flow rate $Q_v/(m^3/h)$	1144.7
Design head $H/m$	17.8
Speed $n/rpm$	1750
Special speed	416
Number of impeller blades $Z_1$	5
Number of guide vane blades $Z_2$	18
Impeller inlet diameter $d_1/mm$	272
Impeller outlet width $b_2/mm$	94
Guide vane inlet width $b_3/mm$	94
Guide vane outlet diameter $d_4/mm$	450

and swirling flow in the calculation of the fluid domain of the nuclear reactor coolant pump, the RNG  $k-\varepsilon$  turbulence model is known to better handle the flow with high strain rate and large curvature of the streamline [14], so the RNG (renormalization group)  $k-\varepsilon$  turbulence model is used. In the iterative calculation process, the total pressure change of the inlet and outlet of the model pump is monitored in real time. When the total pressure change on the monitoring surface of the pump inlet and outlet is less than 1%, the calculation is converged.

**2.4. Boundary Condition.** The boundary condition setting directly determines the accuracy of the solution result. The inlet section is a stationary part, the speed inlet is used, the speed value is calculated according to the rate, the outlet is set to the free outflow, the wall surface adopts no slip condition, the near-wall region is corrective with a standard wall function, and the impeller is set to a rotating reference coordinate system with a rotational speed of 1750 r/min. The calculation medium is boric acid water, and its physical parameters are as follows: temperature  $t = 281^\circ C$ , pressure  $P = 15.5 MPa$ , and density  $\rho = 764.4 kg/m^3$ .

The support at the two radial bearings is set as elastic support of accordance with the actual accident situation. The bearing stiffness and damping coefficient are calculated

using the narrow bearing theory and the Campbell boundary condition. The geometric parameters are set according to the test conditions of the model pump: the oil supply pressure is 1.5 MPa, the speed is 1750 r/min, the lubricating oil density is  $890 kg/m^3$ , and the dynamic viscosity is  $0.048 kg/(m \cdot s)$ . The dynamic grid technique is used to change the eccentricity of the sliding bearing, and the bearing capacity of the bearing under different eccentricities is calculated. The bearing eccentricity under the load is then calculated by the known bearing radial load. Finally, the stiffness and damping coefficients of the oil film model under eccentricity are calculated by applying small displacement and velocity perturbations, respectively.

**2.5. Fluid-Solid Coupling Method.** Previous studies have compared and analyzed the static stress of impellers with unidirectional and bidirectional fluid-solid coupling and found that the unidirectional fluid-solid coupling can meet the static stress analysis of impellers [15]. In this study, the strain, stress distribution, and modal of the impeller of the nuclear reactor coolant pump are analyzed and researched by using the unidirectional fluid-solid coupling method. The coupling process is implemented in ANSYS Workbench. The contact surface between fluid and impeller solid wall is defined as the fluid-solid coupling surface, that is, the front and rear cover of the impeller and blade surface, and inertial load (centrifugal load and gravity load) is applied to the rotor structure.

The static equation for structural strength calculation of the nuclear reactor coolant pump is [16]

$$K\xi = F/\sigma = DB\xi, \quad (1)$$

where  $K$  is a stiffness matrix,  $D$  is an elastic matrix,  $B$  is a strain matrix,  $\xi$  is a displacement,  $F$  is a force, and  $\sigma$  is a stress.

Because the equivalent stress  $\sigma$  extracted from the postprocessing software CFX-Post of ANSYS is defined by the fourth strength theory, the expression is as follows:

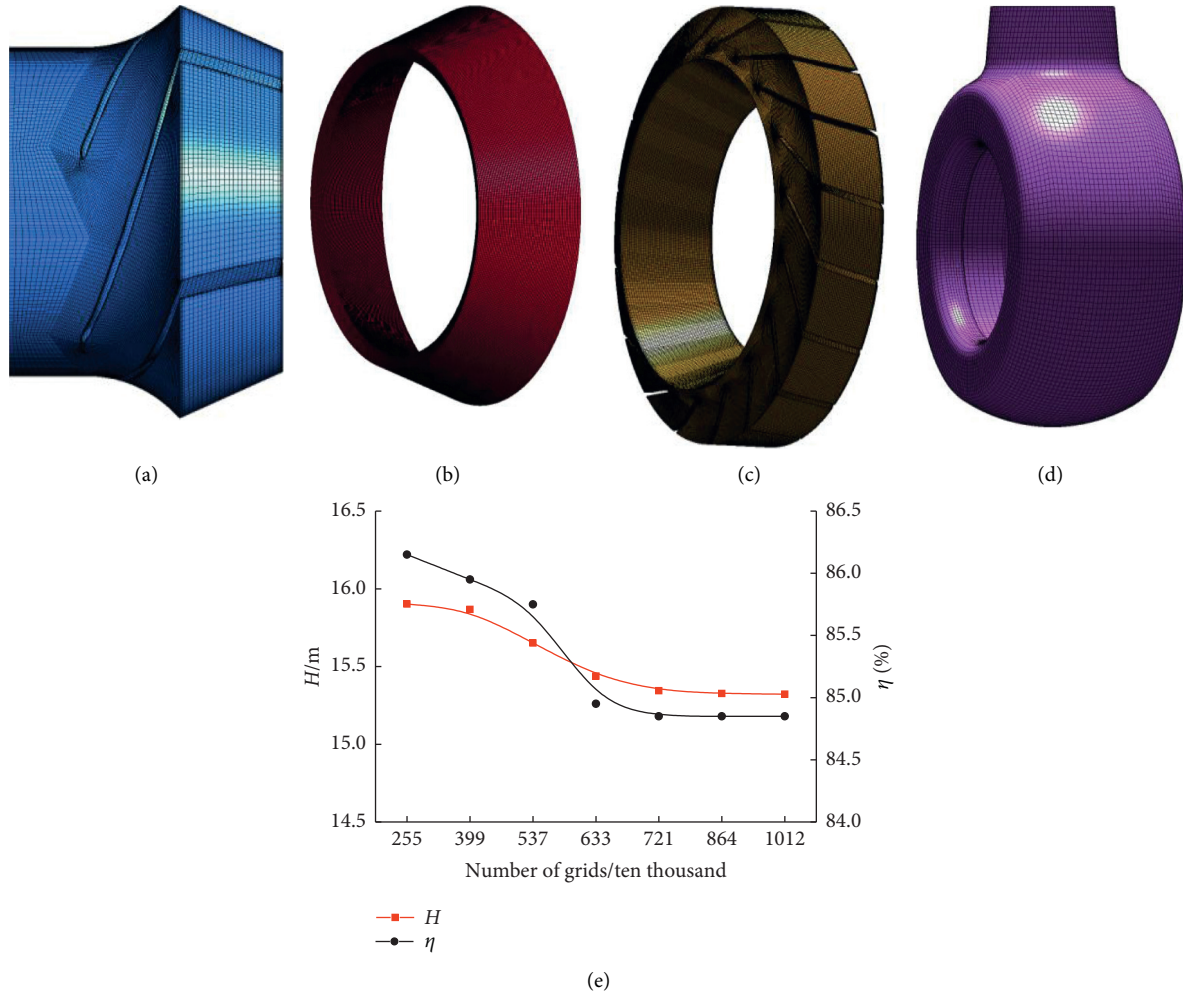


FIGURE 2: Fluid domain grid. (a) Impeller. (b) Stator and rotor clearance. (c) Guide vane. (d) Case. (e) At  $\alpha = 0^\circ$ , simulation values of head and efficiency in different grids.

$$\sigma = \left( \frac{((\sigma_1 - \sigma_2)^2 + (\sigma_2 - \sigma_3)^2 + (\sigma_3 - \sigma_1)^2)}{2} \right)^{1/2} \leq [\sigma], \quad (2)$$

where  $\sigma_1$ ,  $\sigma_2$ , and  $\sigma_3$  are the first, second, and third principal stresses, respectively. Therefore, the equivalent stresses used in this study are calculated according to the fourth strength theory.

### 3. Calculation Results and Analysis

**3.1. Test Verification.** In order to verify the reliability of the numerical calculation results, the numerical calculation results of the model pump are compared with the test results. The results are shown in Figure 3, where  $Q_v$  is the design flow of the model pump. The test bench used is a four-quadrant test bench with a precision level of accuracy. A pressure sensor with an accuracy of  $\pm 0.1\%$  is used to measure the inlet and outlet pressure of the pump. An intelligent electromagnetic flowmeter with an accuracy of  $\pm 1.0\%$  is used for flow measurement, and a torque sensor is used for speed measurement, of which the measuring range is 0–1000N·m and accuracy is  $\pm 0.3\%$ , as shown

in Figure 3(a). In this study, the nuclear reactor coolant pump model was tested with the circumferential angle of the guide vanes  $\alpha = 0^\circ$ . The numerical simulation and test results of this position are shown in Figure 3(b). After the first test, the guide vanes were rotated  $6^\circ$  counterclockwise ( $\alpha = 6^\circ$ ) and a second test was carried out. The simulation and test results are shown in Figure 3(c).

It can be seen from Figure 3(b) that, at  $\alpha = 0^\circ$ , the simulation results of the external characteristics of the model pump have a high consistency with the test results. The test efficiency value of the model pump at the test guarantee point (design condition) is 81.35%, the efficiency value of the simulation at this point is 84.85%, and the relative error between them is 4.3%; the test head value at the test guarantee point is 15.43 m, the simulated head value is 15.34 m, and the absolute error of them is 0.09 m, which is about 0.58% of the test head value. Moreover, with the small flow condition, the simulation value of efficiency is less than the test value and the result of the large flow condition is just the opposite. The relative error between the efficiency test value and simulation value increases slightly, but the relative error does not exceed 7.2%. Because the simulation

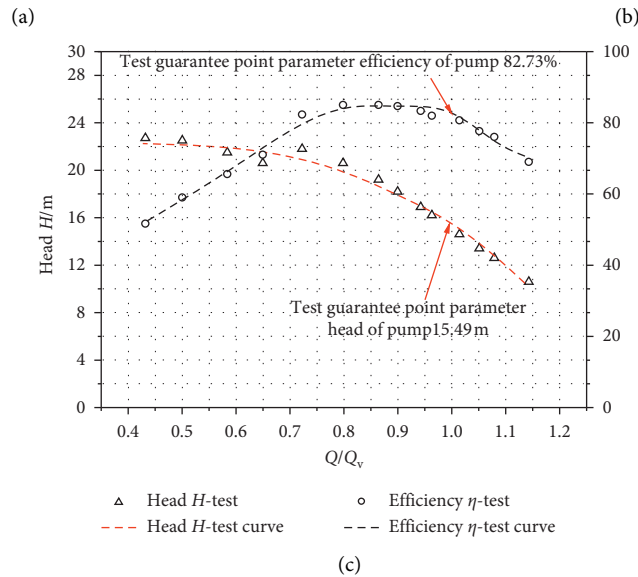
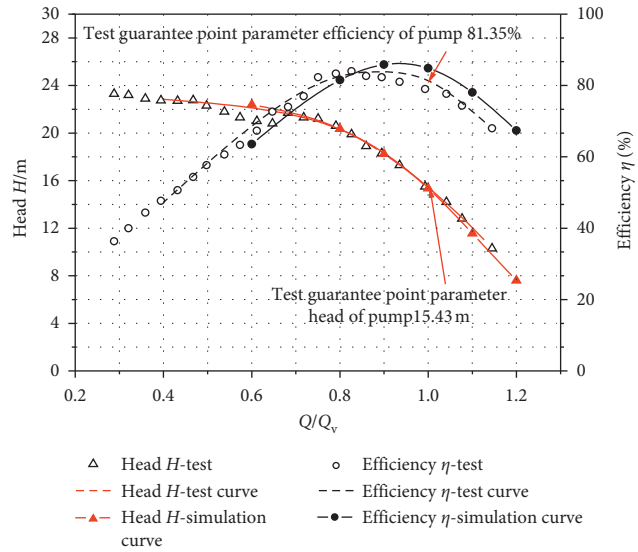


FIGURE 3: Comparison between calculated and experimental values. (a) Test bench. (b) Comparison between calculated and test values when  $\alpha = 0^\circ$ . (c) Test values when  $\alpha = 6^\circ$ .

calculation does not consider the volume loss, mechanical loss, and friction loss at the bearing seal. In general, the physical model and calculation method used in this study can meet the research needs in the calculation accuracy of the range of working conditions in this study. It can be seen from Figure 3(c) that, at  $\alpha = 6^\circ$ , the test efficiency value in the test guarantee point is 82.71% which is 1.36% higher than the test value. Similarly, the test head at  $\alpha = 6^\circ$  in the test guarantee point is 15.49 m which is 0.06 m higher than that at  $\alpha = 0^\circ$ . The above results show that the position of guide vane circumferential placement has a great influence on the efficiency of the nuclear reactor coolant pump.

3.2. Influence of Guide Vane Circumferential Placement Position on the External Characteristics of the Nuclear Reactor Coolant Pump. Figure 4 shows the variation curve of

efficiency and head value of the nuclear reactor coolant pump with circumferential angle of the guide vane. From Figure 4, it can be seen that the variation trend of efficiency and head value of the nuclear reactor coolant pump with guide vane circumferential angle is similar when the nuclear reactor coolant pump of different guide vane circumferential placement positions operates in design conditions. With the increase in the circumferential angle  $\alpha$  of the guide vane, the efficiency and head value increase first and then decrease, and the maximum value appears at the guide vane circumferential placement angle of  $\alpha = 9^\circ$ . The minimum value is located at  $\alpha = 18^\circ$ . The absolute error of the minimum and maximum efficiency is 2.38% and head is 0.56 m which is about 3.1% of the design head. The above phenomenon indicates that the circumferential placement position of the guide vane has a great influence on the efficiency value of the nuclear reactor coolant pump and has little influence on



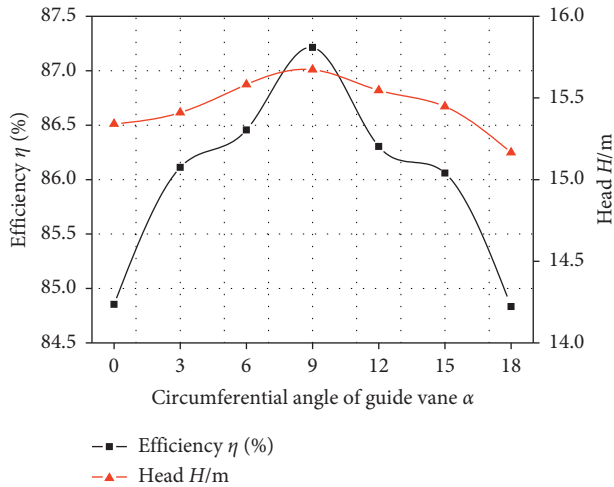


FIGURE 4: The influence of guide vane circumferential placement position on the efficiency and head of the nuclear reactor coolant pump.

the head value. There is an optimal guide vane circumferential placement position.

**3.3. Influence of the Circumferential Arrangement Position of the Guide Vanes on Hydraulic Loss of the Guide Vane and Its Volute.** In order to further study the influence law of the circumferential placement position of the guide vane on the internal flow of the nuclear reactor coolant pump, the hydraulic loss of the guide vane and the volute of the nuclear reactor coolant pump of different guide vane circumferential angles  $\alpha$  are extracted under the design conditions. The result is shown in Figure 5. It can be seen from Figure 5 that, as the circumferential angle of the guide vane changes, the hydraulic loss in the guide vane has only a slight fluctuation, but the hydraulic loss in the volute has a large change, and the change trend is first decreased and then increased. The maximum hydraulic loss in the volute is 0.79 m, the minimum value is 0.39 m, and the fluctuation value is 0.4 m, which accounts for 50.1% of the maximum loss.

In summary, the circumferential placement position of the guide vanes has a greater influence on the internal flow of the volute and the proper placement position of the guide vanes in the circumferential direction can reduce the internal hydraulic loss of the volute. This is mainly because the change of the position of the guide vane in the circumferential direction does not affect the matching of the inlet flow angle of the guide vane with its inlet angle. In other words, the circumferential placement position of the guide vane does not affect the inflow condition of the guide vane inlet; thus, it does not change its internal flow loss. Furthermore, small fluctuations are caused only by the rotor-stator interaction between the impeller and the guide vane. This is because the change in position of guide vane circumferential placement will affect the position of the guide vane runner relative to the diffuser at the outlet of the volute, thus changing the stability of the flow in the volute and thereby affecting its hydraulic loss.

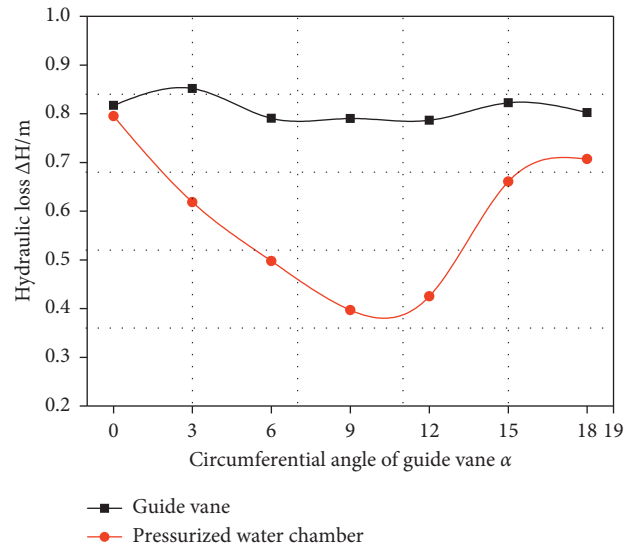


FIGURE 5: The influence of guide vane circumferential placement position on hydraulic loss of the guide vane and its volute.

**3.4. Influence of Guide Vane Circumferential Placement Position on Turbulent Kinetic Energy Distribution.** Figure 6 shows the turbulent kinetic energy distribution in the flow channel of the impeller, guide vane, and volute on the A-A' section (see Figure 1(b)) of the nuclear reactor coolant pump at different locations of guide vanes in the circumferential direction in the design conditions. Because the relative position of the impeller and guide vane varies with time, the position of the impeller is relatively fixed to the outlet diffuser center of the volute and the guide vane is placed in different circumferential positions (see Figures 6(a)–6(g)). The turbulent kinetic energy is not only a measure of the turbulence intensity in the flow but also a sign of flow stability. The higher the turbulent energy value at a certain position in the flow channel, the greater the turbulence intensity at that place and the intense energy exchange, which inevitably leads to greater hydraulic loss. Therefore, the intensity of energy exchange and the concentrated area of hydraulic loss can be seen from the nephogram of turbulent kinetic energy distribution. It can be seen from the circumferential position diagram of the guide vanes shown in Figures 6(a)–6(g) that when the guide vane circumferential angle  $\alpha = 0^\circ$ , the center line of the outlet diffuser of the case just passes the intersection point of the pressure surface of the guide vane blade 1 and the hub of the guide vane. With increase in the guide vane circumferential angle  $\alpha$ , the outlet diffuser center line of the case begins to deflect from the intersection point of suction surface of guide vane blade 2 and hub of the guide vane. When  $\alpha = 0^\circ$ , the center line just reaches the intersection point of guide vane 2 suction surface and hub of the guide vane.

The distribution of turbulent kinetic energy in the annular volute on the A-A' section is now analyzed. As can be seen from Figure 6(a), the high turbulent kinetic energy region in the volute extends from the outlet of guide vane blade 1 to the outlet of the volute and the value of the

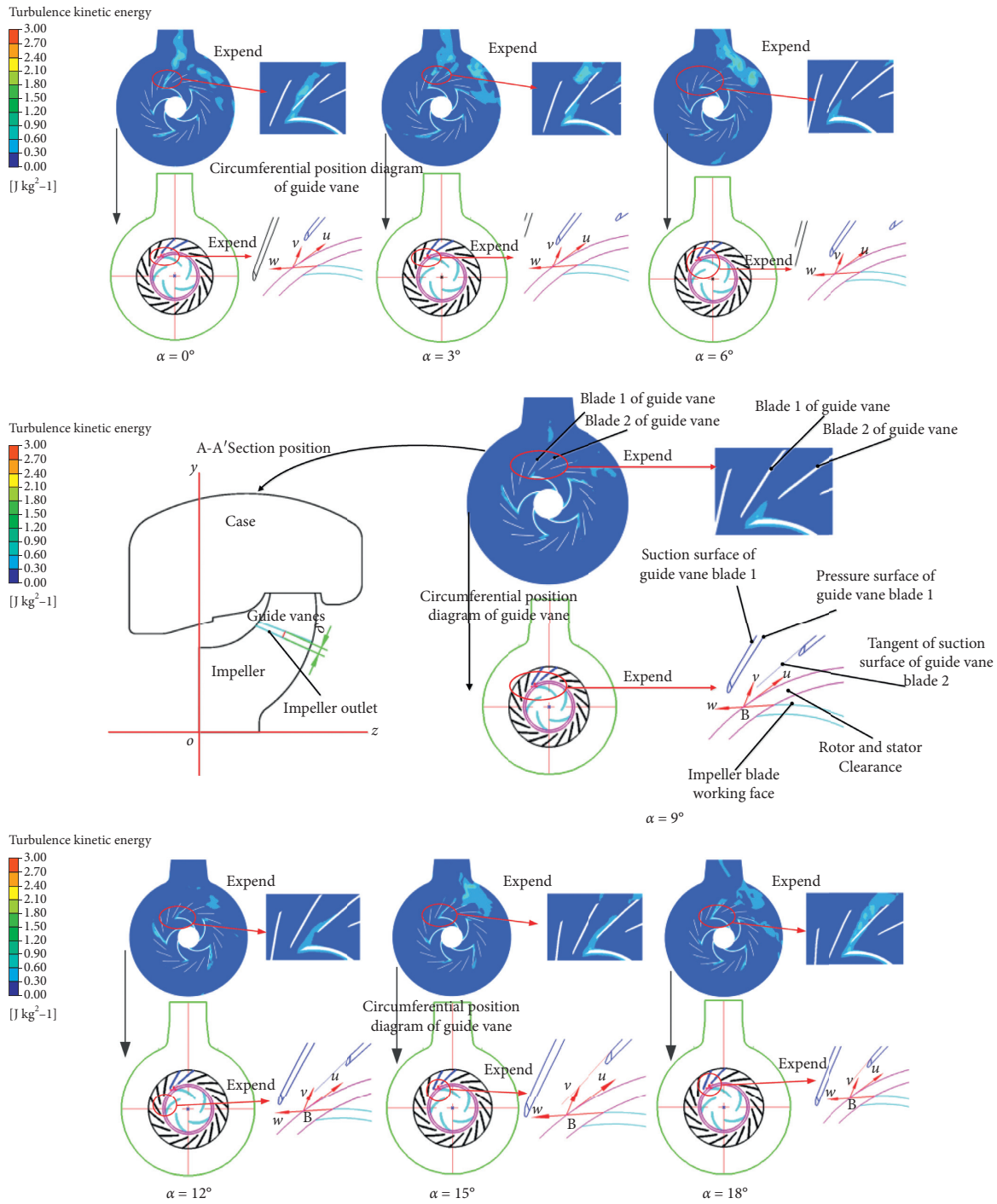


FIGURE 6: Turbulent kinetic energy distribution of the nuclear reactor coolant pump at different guide vane circumferential positions on the A-A' section.

turbulent kinetic energy near the outlet of guide vane blade 1 is relatively high. The distribution area of high turbulent kinetic energy region in Figure 6(b) is larger than that in Figure 6(a), but the value of high turbulent kinetic energy region near the outlet of guide vane blade 1 is lower than that in Figure 6(a). The high turbulent kinetic energy region in Figure 6(c) separates from the outlet of guide vane blade 1 and mainly distributes in the tongue of the case. In Figures 6(d) and 6(e), the distribution area of high turbulent

kinetic energy is smaller and its value is lower. In Figures 6(f) and 6(g), the high turbulent region mainly distributes from the lower side of the tongue to the outlet of the corresponding blade. However, in Figure 6(f), the high turbulent region has a higher value and a more concentrated area than Figure 6(g). The above phenomena show that the distribution position, value, and distribution area of the high-turbulence zone in the case are all changed with the position of the guide vane in the circumferential direction. When the

guide vane circumferential angle  $\alpha = 9^\circ$  (i.e., the outlet center line of the case is just located at the center of the outlet of the guide vane channel), the area of high turbulent kinetic energy distribution in the volute is smaller and the value is lower. This further shows that the flow in the volute is more stable and the loss is lowest when the outlet diffuser center line of the volute is located at the outlet center of the guide vane channel, which is also consistent with the analysis result of the hydraulic loss curve in the volute in Figure 5.

The position of point B in Figure 6 is the intersection of the outlet tangent of impeller blade working face and the shroud of the guide vane, and its position is related to the outlet diffuser center of the case and independent of the position of the guide vane. It can be also seen from Figure 6 that no matter how the circumferential position of the guide vane is arranged, there exists a high turbulent kinetic energy region on the back of the impeller blade and at the outlet of the impeller blade. This is mainly due to the finite number of blades of the impeller, so that there is an axial vortex in the impeller flow path. Axial vortices accelerate the flow velocity on the back of the blade and generate vortices at the outlet of the blade, i.e., the wake phenomenon of the rotor blade, which shows a high turbulent region in the turbulent kinetic energy nephogram. At the same time, it can be seen that the shape and size of the high-turbulence zone at the outlet of the impeller blade vary with the position of guide vane circumferential placement. The variation law is as follows: when the guide vane circumferential angle  $\alpha$  changes from small to large in the range of  $0^\circ \sim 9^\circ$ , the high turbulence kinetic energy zone decreases and the length decreases along the direction of absolute velocity at point B. When the circumferential angle of the guide vane  $\alpha$  changes from small to large in the range of  $9^\circ \sim 18^\circ$ , the change trend of the turbulent kinetic energy zone is opposite to that of  $\alpha$  at  $0^\circ \sim 9^\circ$ . The above phenomena show that the change of guide vane circumferential placement position will affect the flow state and shape of impeller blade wake at point B.

The reason is as follows: as can be seen from the speed triangle in Figure 6, when the impeller is rotated to a fixed position (the tangent to the outlet of the blade working face passes through point B), the velocity and direction of the fluid at point B are the same. However, because of the difference in the circumferential position of the guide vanes, the absolute velocity direction of the fluid at point B and the spatial relative position of blade 1 of guide vanes are changed. As shown in Figure 6(a), the direction of the absolute velocity of the fluid at point B refers to the inlet of guide vane blade 1, indicating that when the guide vane circumferential angle  $\alpha = 0^\circ$ , the wake of the blade at point B will directly impinge on the inlet of guide vane blade 1, further disturbing the flow field at the inlet of blade 1 of the guide vane. Conversely, the disturbed flow field will affect the wake of the rotor blade at point B, reinforcing the rotor-stator interaction effect at that point, as shown in Figure 6(a). In Figures 6(c) and Figure 6(d), the absolute velocity direction of the fluid at point B points to the center of the guide vane flow channel, indicating that when the guide vane is placed at a circumferential angle of  $\alpha = 6^\circ \sim 9^\circ$ , the wake of the rotor blade at point B, not affected by the interference of the

guide blade, will maintain its original flow state. The rotor-stator interaction effect is the weakest, the area of the high-turbulence region is the smallest, and the value is low. In Figures 6(f) and 6(g), the absolute velocity direction of the fluid at point B is located below the tangent of the suction surface of blade 2 of the guide vane, indicating that when the guide vane circumferential angle  $\alpha = 15^\circ \sim 18^\circ$ , the wake of the rotor blade at point B will be affected by the suction surface of blade 2 of the guide vane and the rotor-stator interaction effects will be enhanced.

### 3.5. Influence of Guide Vane Circumferential Placement Position on the Statics of Its Blades, Shroud, and Hub.

Figure 7 is a diagram of the guide vane structure. The material is duplex stainless steel 2570. The allowable stress at design temperature is 227.5 MPa. Figure 8 shows the influence curve of change of the guide vane circumferential angle on the maximum equivalent stress and total deformation on the pressure and suction surfaces of the guide vane. From Figure 8, it can be seen that the maximum equivalent stress on the guide vane pressure surface varies with the increase in the guide vane circumferential angle, but the change trend is not obvious. When the guide vane circumferential angle  $\alpha = 6^\circ$ , the maximum equivalent stress on the pressure surface shows the maximum value, and when  $\alpha = 3^\circ$ , the minimum value appears, the difference between them is 0.444 MPa, accounting for about 3.2% of the maximum value. With the increase of the guide vane circumferential angle, the maximum equivalent stress on the suction surface increases first and then decreases, and the maximum value appears at  $\alpha = 15^\circ$  while the minimum value appears at  $\alpha = 0^\circ$ . The difference between them is 0.585 MPa, accounting for about 7.9% of the maximum value. The results show that the circumferential placement position of the guide vane has a great influence on the maximum equivalent stress of the suction surface of the guide vane. When the center of the volute outlet diffuse channel is closer to the outlet of the suction surface of the guide vane (as shown in Figure 6(f), the outlet diffuser center line of the case is close to the outlet of the suction surface of guide vane blade 2 when  $\alpha = 15^\circ$ ), the maximum equivalent stress on the suction surface of the guide vane becomes greater.

It can also be seen from Figure 8 that the maximum total deformations on the pressure and suction surfaces of the guide vane have the same trend with the increase in the guide vane circumferential angle. The maximum deformations increase at first and then decrease. The maximum deformations occur at  $\alpha = 15^\circ$ , and the minimum deformations occur at  $\alpha = 0^\circ$ . The difference between the maximum and minimum deformations on pressure surfaces is  $1.176 \mu\text{m}$ , accounting for 18.9% of pressure surface maximum deformations, and is  $1.148 \mu\text{m}$  on suction surfaces, accounting for 21.9% of suction surfaces maximum deformations. This shows that the position of the guide vane in the circumference direction has a great influence on the maximum total deformation of the pressure and suction surfaces of the guide vane. When the center line of the outlet diffuser channel of the volute is closer to the exit edge of the suction surface of



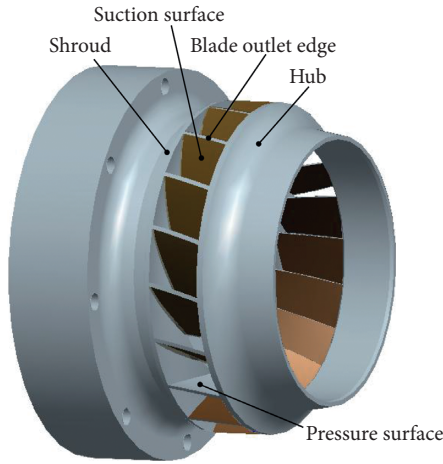


FIGURE 7: Schematic diagram of guide vane structure.

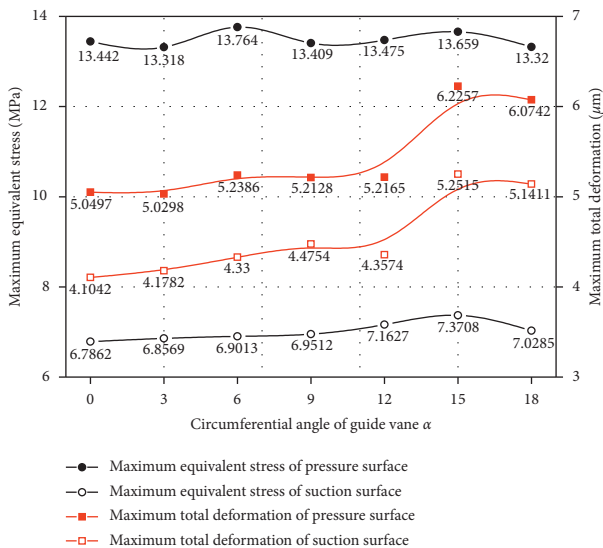


FIGURE 8: The influence of guide vane circumferential placement position on guide vane statics.

the guide vane, the value of the maximum total deformation of the guide vane blade is larger.

Figure 9 shows the contour of equivalent stress and total deformation distribution on the pressure and suction surfaces of guide vanes at  $\alpha = 9^\circ$  in the design condition. From Figure 9, it can be seen that there is a phenomenon of stress concentration on the pressure and suction surfaces of guide vanes, and the maximum equivalent stress occurs at the junction of the guide vane outlet edge and the shroud. From the contour of equivalent stress on the pressure surface, it can be seen that equivalent stress distributed at the outlet edge of the guide vane is obviously higher than that distributed at the blade inlet edge, and the value of equivalent stress near the shroud and hub is obviously higher than that in the middle of the blade. The distribution of equivalent stress on the suction surface of the blade is similar to that on the pressure surface of the blade. The above phenomena show that the outlet edge of the guide vane and the junction

with shroud and hub are high stress concentration areas, and the junction position between the outlet edge and shroud and hub is the most vulnerable place to strength damage. This is because the static pressure at the outlet of the guide vane is larger than that at the inlet. Because of the function of reducing speed and boosting pressure of the guide vane, the equivalent stress at the outlet is higher than that at the inlet. Equivalent stress values in the area of contact with shroud and hub are higher than those in the middle area of blades. Because the restraint of the shroud and hub prevents the guide vane blade from effectively releasing stress through deformation, it is easy to cause stress concentration.

From Figure 9, it can also be seen that the distribution law of total deformation on the pressure surface and suction surface of the blade is basically similar. In the middle of the outlet edge of the blade is the maximum area of total deformation, and the total deformation near the shroud is higher than that near the hub. The above phenomena show that the blade exit edge and the area near the shroud are vulnerable to stiffness damage. This is mainly due to the large static pressure and thinner thickness at the exit edge of the blade compared with the inlet edge. Therefore, the deformation of the blade exit edge is large. Because the contact area of the blade and shroud is smaller than that of the hub, the deformation of the shroud contact area is larger than that of the hub under the same stress condition.

Figure 10 shows the influence of guide vane circumferential placement position on the maximum equivalent stress and maximum total deformation of the shroud and hub in design conditions. Figure 10 shows that the maximum equivalent stress of the shroud and hub of the guide vanes varies with the increase in their circumferential angles. The maximum equivalent stress of the shroud appears at  $\alpha = 9^\circ$ , and the minimum value appears at  $\alpha = 0^\circ$ . The difference between them is 0.563 MPa, which accounts for about 4.3% of the maximum value. The maximum equivalent stress of the hub appears at  $\alpha = 3^\circ$ , and the minimum value appears at  $\alpha = 6^\circ$ . The difference between them is 1.018 MPa, accounting for about 10.3% of the maximum value. The above phenomena show that the circumferential placement position of guide vanes has a greater impact on the maximum equivalent stress of the hub and a smaller impact on the shroud. It can also be seen from Figure 10 that the variation trend of the maximum total deformation of the shroud and hub is basically similar. The maximum total deformation of the shroud occurs at  $\alpha = 12^\circ$ , and the minimum occurs at  $\alpha = 3^\circ$ . The difference between them is 0.082  $\mu\text{m}$ , accounting for about 4.8% of the maximum. The relative error of the maximum total deformation of the hub is 3.6%. It can be seen that the circumferential placement position of the guide vane has little influence on the maximum total deformation of the shroud and hub.

Figures 11 and 12, respectively, show distribution contour of the equivalent stress and total deformation on the shroud and hub in design conditions at  $\alpha = 9^\circ$ . It can be seen in Figure 10 that the equivalent stress distribution of the shroud and hub shows the stress concentration phenomenon and the equivalent stress distribution in each channel is similar. The equivalent stress mainly concentrates on the

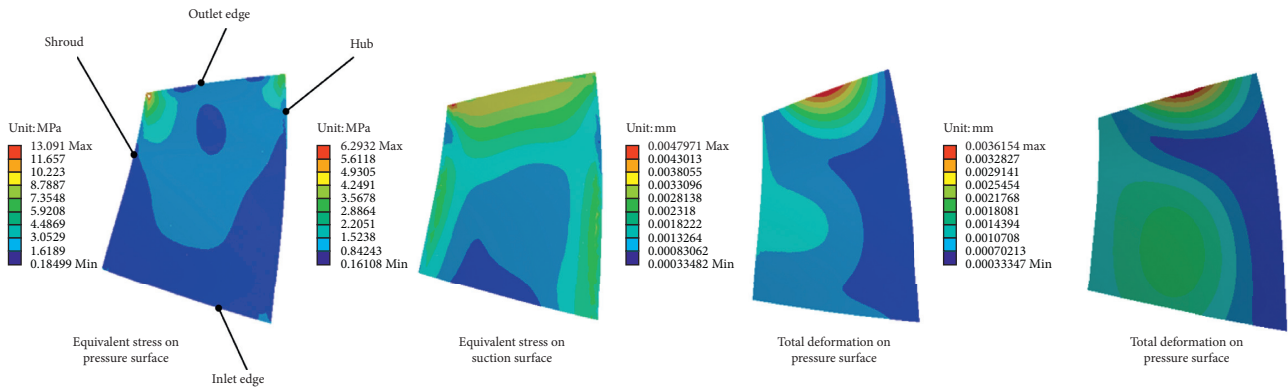


FIGURE 9: Distribution of equivalent stress and total deformation on the guide blade.

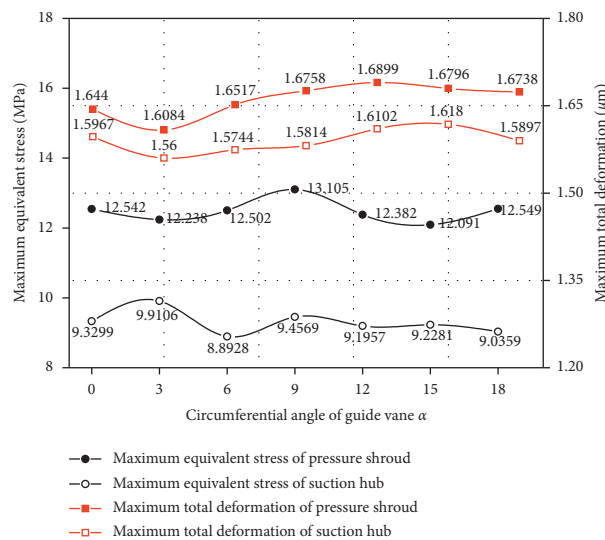


FIGURE 10: The influence of the circumferential position of the guide vane on the statics of the shroud and hub of the guide vane.

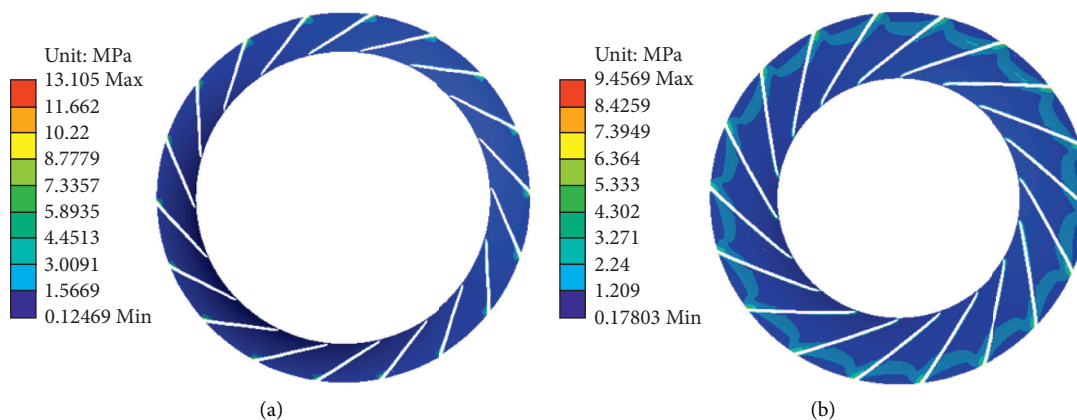


FIGURE 11: Equivalent stress distribution on (a) the shroud and (b) the hub.

shroud at the contact position between the pressure surface outlet of the blade and the shroud. The main concentration area of the hub is the outlet guide vane runner from the contact position between the pressure surface outlet of the guide vane and the hub to the end of the suction surface of

another guide vane blade, which is crescent-shaped. The above phenomena show that the contact position between the outlet edge of the guide vane pressure surface and the shroud and hub is the most vulnerable place to strength damage. This is mainly due to the double restrictions of the

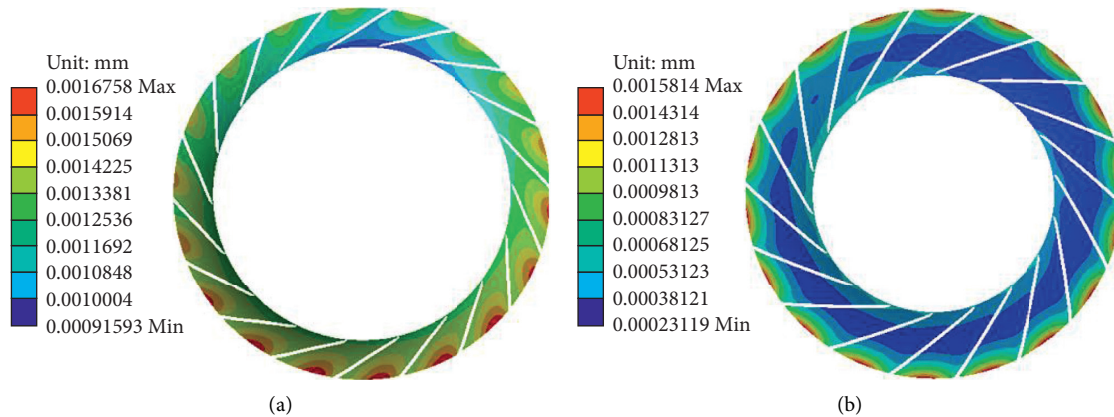


FIGURE 12: Distribution of total deformation on (a) the shroud and (b) the hub.

guide vane, the shroud, and the hub in the region, making the stress release not easy. From Figure 12, it can be seen that the larger total deformation area of shroud and hub occurs near the center of the flow channel. The difference is that the total deformation in the guide vane channel near the diffuser channel of the volute on the shroud is obviously smaller than that in the guide vane channel at other locations, and the distribution of the hub is more even. The reason is that the guide vane channel near the diffuser channel of the case is greatly affected by the volute, and the high-pressure liquid is easy to evacuate, so the total deformation is small.

#### 4. Conclusion

In this study, the influence of the circumferential placement position of the guide vane of the nuclear reactor coolant pump on its internal flow field, stress, and strain is studied by means of the one-way fluid-structure coupling numerical calculation method and test results. The following conclusions are drawn:

- (1) The position of guide vane circumferential placement has a great influence on the efficiency of the nuclear reactor coolant pump near small flow rate and design condition, but has a weak effect at large flow rate. However, the influence on its head is just the opposite. The appropriate position of guide vane circumferential placement is conducive to improving the hydraulic performance of the nuclear reactor coolant pump.
- (2) In design condition, the position of guide vane circumferential placement has significant influence on the efficiency of the nuclear reactor coolant pump and the maximum equivalent stress of the suction surface of the guide vane and hub, but has little influence on the head value and the maximum equivalent stress of pressure surface and shroud. Also, there is an optimal position of guide vane circumferential placement.
- (3) When the outlet diffuser center of the volute is located at the outlet center of the guide vane channel, the flow in the case is the most stable, which can

reduce internal loss. The change of the position of the guide vane in the circumferential direction will affect the flow pattern and shape of the rotor blade wake at the outlet of the impeller blade.

- (4) The junction of the guide vane outlet and the shroud and hub is a high stress concentration area, and the junction of the guide vane outlet and shroud is the most vulnerable area to strength failure.

#### Data Availability

The key parameters of the nuclear reactor coolant pump related to the research content have been given in the manuscript, and all the parameters, test reports, and related information submitted are authentic and effective in this manuscript.

#### Conflicts of Interest

The authors declare that they have no conflicts of interest.

#### Acknowledgments

This work was supported by the Natural Science Foundation of China (no. 51469 013).

#### References

- [1] J. Deng, J. Lu, Y. Xu et al., "Effect of clocking position of front guide vane on pulsation characteristic of pressure in centrifugal pump," *Journal of Northwest A & F University (Natural Science Edition)*, vol. 44, no. 1, pp. 217–222, 2016.
- [2] J. Lu, J. Deng, Y. Xu et al., "Effect of clocking position of inducer on hydraulic characteristics of centrifugal pump," *Transactions of the Chinese Society of Agricultural Engineering (Transactions of the CSAE)*, vol. 31, no. 19, pp. 54–60, 2015.
- [3] B. Zhao, Ce Yang, Li Du et al., "The influence of frequency and clocking on stator wake in an axial-radial combined compressor," *Journal of Engineering Thermophysics*, vol. 34, no. 2, pp. 245–248, 2013.
- [4] X. Cheng, B. Xu, X. Ye et al., "Influence of circumferential setting position of vaned diffuser on radial thrust of impeller in nuclear reactor coolant pump," *Journal of Lanzhou University of Technology*, vol. 44, no. 4, pp. 52–59, 2018.

- [5] X. Cheng, C. Jia, C. Yang et al., "Influence of circumferential position of guide vane on unsteady flow characteristics in nuclear reactor coolant pump," *Journal of Mechanical Engineering*, vol. 52, no. 16, pp. 197–204, 2016.
- [6] R. Liu and Z. Xu, "Effect of the splitter blade position on the characteristic of high-speed centrifugal compressor," *Acta Aerodynamica Sinica*, vol. 23, no. 1, pp. 129–134, 2005.
- [7] A. Posa, R. A. Lippolis, and E. Balaras, "Large-eddy simulations in mixed-flow pumps using an immersed-boundary method," *Computers & Fluids*, vol. 47, no. 1, pp. 33–43, 2011.
- [8] D. Q. Yuan, H. Yan, and P. P. Wang, "Impact of diffuser width on the performance of AP1000 reactor coolant pump," *Advanced Materials Research*, vol. 516–517, pp. 921–925, 2012.
- [9] W. N. Jin, R. Xie, M. T. Hao et al., "Influence of guide vane wrap angle key design parameters on hydraulic performance of nuclear reactor coolant pump," *Applied Mechanics & Materials*, vol. 721, pp. 73–77, 2014.
- [10] A. Poullikkas, "Two phase flow performance of nuclear reactor cooling pumps," *Progress in Nuclear Energy*, vol. 36, no. 2, pp. 123–130, 2000.
- [11] Y. Li, R. Li, X. Wang et al., "Scaling effect for hydraulic performance prediction of nuclear reactor coolant pump," *Atomic Energy Science and Technology*, vol. 49, no. 4, pp. 609–615, 2015.
- [12] J. Tang, *Concise Mechanical Design Manual*, Shanghai Science and Technology Publishing House, Shanghai, China, 3 edition, 2000.
- [13] X. Cheng, L. ü Boru, X. Zhang et al., "Influence of outlet edge position of guide vane on performance of well submersible pump," *Transactions of the Chinese Society of Agricultural Engineering (Transactions of the CSAE)*, vol. 34, no. 10, pp. 68–75, 2018.
- [14] H. Liu, D. Liu, Y. Wang et al., "Applicative evaluation of three cavitating models on cavitating flow calculation in centrifugal pump," *Transactions of the Chinese Society of Agricultural Engineering*, vol. 28, no. 16, pp. 54–59, 2012.
- [15] H. Liu, H. Xu, X. Wu et al., "Effect of fluid-structure interaction on internal and external characteristics of centrifugal pump," *Transactions of the Chinese Society of Agricultural Engineering*, vol. 28, no. 13, pp. 82–87, 2012.
- [16] D. L. Sondak and D. J. Doeney, "Simulation of coupled unsteady flow and heat conduction in turbine stage," *Journal of Propulsion & Power*, vol. 16, no. 6, pp. 1141–1148, 2015.